Robust controlled formation of Turing patterns in three-component systems

Maxim Kuznetsov [*]
Division of Theoretical Physics, P.N. Lebedev Physical Institute of the Russian Academy of Sciences, Moscow 119991, Russia and Nikolsky Mathematical Institute, Peoples Friendship University of Russia (RUDN University), Moscow 117198, Russia

(Received 30 September 2021; accepted 4 January 2022; published 13 January 2022)

Over the past few decades, formation of Turing patterns in reaction-diffusion systems has been shown to be the underlying process in several examples of biological morphogenesis, confirming Alan Turing's hypothesis, put forward in 1952. However, theoretical studies suggest that Turing patterns formation via classical "short-range activation and long-range inhibition" concept in general can happen within only narrow parameter ranges. This feature seemingly contradicts the accuracy and reproducibility of biological morphogenesis given the stochasticity of biochemical processes and the influence of environmental perturbations. Moreover, it represents a major hurdle to synthetic engineering of Turing patterns. In this work it is shown that this problem can be overcome in some systems under certain sets of interactions between their elements, one of which is immobile and therefore corresponding to a cell-autonomous factor. In such systems Turing patterns formation can be guaranteed by a simple universal control under any values of kinetic parameters and diffusion coefficients of mobile elements. This concept is illustrated by analysis and simulations of a specific three-component system, characterized in absence of diffusion by a presence of codimension two pitchfork-Hopf bifurcation.

DOI: 10.1103/PhysRevE.105.014209

I. INTRODUCTION

In 1952, Alan Turing suggested that the key to many events of morphogenesis, i.e., formation of organs in living organisms, should be the instability of a spatially homogeneous state in a system of interacting and diffusing chemicals, leading to their inhomogeneous distributions and subsequent different local effects on cell behavior throughout the tissue [1]. Turing's theory has been used in a variety of different studies—not only biological [2–4] and purely mathematical [5–7] but also physical [8–10], chemical [11–13], and even sociological [14–16]. The general form of reaction-diffusion systems considered in these studies can be presented as:

$$\dot{\mathbf{u}} = A(\mathbf{u} - \mathbf{u_0}) + Q + D\Delta\mathbf{u}, \tag{1}$$

where $\mathbf{u} = (u_1, u_2, \dots, u_N)^T$ is the vector of N variables; $\mathbf{u_0}$ is the considered uniform stationary state, stable in the absence of diffusion; $A = a_{ij}$ $(i, j = 1, 2, \dots, N)$ is the Jacobian of the system, linearized at $\mathbf{u_0}$; $D = I_N(D_1, D_2, \dots, D_N)^T$ is the diagonal matrix of diffusion coefficients; and Q is the vector of nonlinear terms.

Turing derived the conditions for the instability that leads to the formation of stationary patterns in two-component systems. These conditions can be represented the following way, where two first equations guarantee the stability of $\mathbf{u_0}$ in absence of diffusion:

$$\begin{aligned} -a_{11} - a_{22} &> 0,\\ a_{11}a_{22} - a_{12}a_{21} &> 0,\\ D_2^2a_{11}^2 + D_1^2a_{22}^2 &> 2D_1D_2(a_{11}a_{22} - 2a_{12}a_{21}). \end{aligned}$$

In particular, these inequalities infer that one of the elements, e.g., the first one, should stimulate its own production near $\mathbf{u_0}$, i.e., $a_{11} > 0$, while another element should act in the opposite way, i.e., $a_{22} < 0$, and should have a greater diffusion coefficient, i.e., $D_2 > D_1$.

These conditions restrict the values of Jacobian elements and diffusion coefficients in a way, which is associated with two problems that are crucial at least in the context of biological systems, i.e., the requirements of *differential diffusivity* and *fine-tuning* of parameters. That is, the condition $D_2 > D_1$ has to hold, and under any selected values of diffusion coefficients the range of Turing instability in the space of kinetic parameters represents a bounded region whose volume becomes increasingly small as $D_2 \to D_1$. However, given the specificity of the morphogens' tasks, it is reasonable to expect them to be mainly large proteins (which most of the suggested morphogenes indeed are [17]), which thus should have close values of intrinsic diffusion coefficients under similar conditions. Furthermore, the rates of kinetic interactions in tissues should depend on stochastic processes, including gene expression, as well as on external conditions, which should lead to spatiotemporal as well as interindividual variability in kinetic parameters in living organisms. Despite this, patterning processes in nature are remarkably precise and reproducible, even under significant environmental perturbations. Viable, albeit obviously altered, organisms can develop even under high radiation exposure (of dozens of Grays), which induces phenotypic changes during ontogenesis (see, e.g., Ref. [18]).

Furthermore, requirements of differential diffusivity and fine-tuning have led to the fact that Turing patterns are extremely difficult to engineer in biological synthetic networks [17], which may have potential application, e.g., in regenerative medicine. At that, Turing patterns engineering is a quite

*kuznetsovmb@mail.ru

feasible task in chemical frameworks, in which uncertainty in parameter values is low.

Several ideas have been produced that aim to increase the *robustness* of Turing patterns formation, i.e., the tolerance of a pattern-generating system to the alterations of parameters. The earliest idea of this kind is the introduction of reversible binding of an activator with an immobile element. The effect of such a mechanism can roughly correspond to the decrease of activator's diffusion coefficient, which thus increases the kinetic region that provides Turing patterns [19]. This method allowed experimental confirmation of Turing's hypothesis in a chemical system in 1990 [20] and to implement the first synthetic mechanism, leading to disordered patterns in mammalian cells in 2018 [21]. The use of a small inorganic molecule as long-range inhibitor has also been suggested in a rather specific potential mechanism that should give rise to Turing patterns in synthetic bacterial population [22].

Further, it has been noticed that the relative range of parameters, leading to Turing patterns, increases with the increase of number of system's components [23]. Moreover, for stochastic systems it was shown that generation of time-dependent patterns with large amplitude can happen outside the parameter range that provides deterministic Turing patterns [24]. Also in 2018, stochastic Turing patterns were obtained in a genetically engineered synthetic bacterial population [25].

Such modifications alleviate the problems of differential diffusivity and fine-tuning but do not exclude them. Significant results in tackling these problems have been achieved in theoretical works that study the systems with preassigned fixed *network structures* [26–29]. These are the sets of interactions between the system's elements, each of which can be activating, inhibiting, or absent. A network structure thus corresponds to the set of signs of elements of matrix A in Eq. (1). Importantly, it does not determine their absolute values, which correspond to the strengths of interactions. In the corresponding studies they are varied in large ranges. The work [26] demonstrated the existence of three-component systems with one immobile element, i.e., having zero diffusion coefficient, that can produce Turing patterns under any positive values of diffusion coefficients of the two remaining elements, thus overcoming the need for their differential diffusivity but maintaining the need for fine-tuning of the kinetic values. Notably, from the biological point of view, the case of zero diffusion coefficient differs qualitatively from the case of very small but finite diffusion coefficients—immobile elements correspond to factors that do not leave an individual cell and can perform its function only inside it, e.g., transcription factors or elements of signaling pathways. Some network structures, able to overcome differential diffusivity, turned out to be more robust than others; however, it was shown that none of them by itself can guarantee Turing patterns formation. On the contrary, in Ref. [29] all network structures were demonstrated to be highly sensitive to perturbations of parameters.

In this work it is shown that certain network structures allow overcoming the problems of fine-tuning and differential diffusivity by allowing the selection of a control parameter, continuous increase of which will eventually result in Turing instability of the uniform stationary state under any values of kinetic parameters and diffusion coefficients, with no other instabilities being present. Analysis and numerical simulations are performed that suggest the existence of systems in which in the presence of external noise such a method should almost always lead to the formation of stationary patterns within a reasonable time window, except for the certain regions of rather extreme parameter variation.

II. SEARCH FOR NETWORKS CAPABLE OF ROBUST TURING PATTERNS FORMATION

In this work the systems that correspond to the general form of Eqs. (1) are considered with $N = 3$ components. The full linear analysis in the general case with explicit conditions for Turing instability can be found in our previous work [30]. Herein only crucial moments are briefly recalled, related to the special case of the system with one immobile element: $D = I(D_1, D_2, 0)^T$, $D_1 > 0$, $D_2 > 0$. The position of the uniform stationary state $\mathbf{u_0}$ is considered to be independent of parameters values for simplicity.

In the one-dimensional (1D) case an infinitesimal perturbation that represents a sinusoidal wave with wave number k evolves in linear approximation as $\sum_{j=1}^{3} \alpha_j \mathbf{v_j} e^{ikr} e^{\lambda_j(k)t}$, where α_j are the coordinates of initial perturbation with respect to the basis of eigenvalues $\mathbf{v_j}$ and $\lambda_j(k)$ are in general case complex numbers that characterize the evolution of corresponding components. Inserting this formula into the linearized version of Eq. (1) provides the explicit equation for eigenvalues and eigenvectors $[A - \lambda(k)I - k^2 D]\mathbf{v} = 0$. Eigenvectors can be nonzero if and only if the so-called *dispersion relation* holds, which for the considered case is

$$\begin{vmatrix} a_{11} - k^2 D_1 - \lambda(k) & a_{12} & a_{13} \\ a_{21} & a_{22} - k^2 D_2 - \lambda(k) & a_{23} \\ a_{31} & a_{32} & a_{33} - \lambda(k) \end{vmatrix} = 0. \tag{2}$$

This relation allows us to find eigenvalues corresponding to every wave number k. If all of them have negative real parts, then any infinitesimal perturbation will die out. If for some k at least one of eigenvalues has positive real part, then the corresponding perturbation will grow, indicating one of the diffusion instabilities. A positive real eigenvalue corresponds to Turing instability, leading to stationary patterns. Two complex conjugate eigenvalues with positive real part correspond to wave instability (that is impossible in two-component case), which yields autowaves right after its onset [31]. Note that since the dispersion relation depends only on the norm of wave vector k, it is as well valid for any dimensionality of space due to the rotational symmetry of spatially homogeneous systems.

A. Eliminating the need for differential diffusivity

As $k \to \infty$, Eq. (2) can be presented as

$$k^4 D_1 D_2 [a_{33} - \lambda(k)] + o(k^4) = 0,$$

and therefore one of its solutions tends to a_{33}. If a_{33} is positive, then the waves within an infinite range of wave numbers, including infinitesimal wavelengths, are unstable, and the critical eigenvalue tends asymptotically to a_{33} for large wave numbers. Notably, an analogous situation emerges in classical two-component activator-inhibitor systems under an infinite disparity between diffusion coefficients of its elements. Importantly, it does not lead to the formation of stable Turing patterns. It was shown that in continuous space the solutions of such systems are unstable [32], while in discretized space, which may correspond to biological cells, an initial noisy prepattern evolves to form a stationary "salt-and-pepper" pattern with a characteristic wavelength equal to the minimal of those that spatial discretization can reproduce [28]. This feature has been noticed already in Turing's seminal paper in the context of cells [1].

The case of $a_{33} = 0$, however, is qualitatively different and thus presents certain interest and will be considered from now on.

Dispersion relation (2) can be rewritten as $\lambda(k)^3 - \sigma(k)\lambda(k)^2 + \Sigma(k)\lambda(k) - \Delta(k) = 0$, where, taking into account $a_{33} = 0$:

$$\begin{aligned}\sigma(k) &\equiv \sigma_0 - k^2[D_1 + D_2],\\ \Delta(k) &\equiv \Delta_0 + k^2[D_1 a_{23}a_{32} + D_2 a_{13}a_{31}],\\ \Sigma(k) &\equiv \Sigma_0 - k^2[D_1 a_{22} + D_2 a_{11}] + k^4 D_1 D_2.\end{aligned} \tag{3}$$

Here σ_0 is the trace of matrix A, Δ_0 is its determinant, and Σ_0 is the sum of its principal minors.

The Routh-Hurwitz stability criterion [33] provides the following conditions for the absence of diffusion instabilities, where the relations between the coefficients of dispersion relation and its roots are accounted for:

$$\begin{aligned}\forall k\ \ \sigma(k) &= \lambda_1(k) + \lambda_2(k) + \lambda_3(k) < 0,\\ \Delta(k) &= \lambda_1(k)\lambda_2(k)\lambda_3(k) < 0,\\ \sigma(k)\Sigma(k) - \Delta(k) &\\ &= [\lambda_1(k)+\lambda_2(k)][\lambda_1(k)+\lambda_3(k)][\lambda_2(k)+\lambda_3(k)]\\ &< 0.\end{aligned} \tag{4}$$

For $k = 0$ these conditions are assumed to be met, since they correspond to the spatially uniform case. As k is increased, violation of the second condition, while the third is met, implies the change of sign of the real part of one eigenvalue and thus indicates the onset of Turing instability. Analogically, violation of the third condition means the onset of wave instability. The first condition cannot be violated, as $\sigma(k)$ is a decreasing function of k.

According to Eqs. (3), if $a_{13}a_{31}$ and $a_{23}a_{32}$ are non-negative with at least one of them positive, then $\Delta(k)$ nullifies at one and only one value of positive wave number k. If no wave instability is manifested simultaneously, then the plot of the critical eigenvalue looks at a qualitative level as depicted in Fig. 1. In this case the waves within an infinite range of wave numbers are unstable and their linear rate of growth tends to zero for infinitesimal wavelengths. This feature is maintained under any positive values of D_1 and D_2, thus formally not requiring differential diffusivity.

Contrary to the case of $a_{33} > 0$, such type of Turing instability can lead to the formation of classical Turing patterns in response to small perturbations of the uniform stationary state, as was demonstrated in Ref. [30]. This is due to the fact that the waves with smaller wavelengths should grow increasingly slower in linear approximation. Therefore they merely should not have time to significantly influence the process of pattern

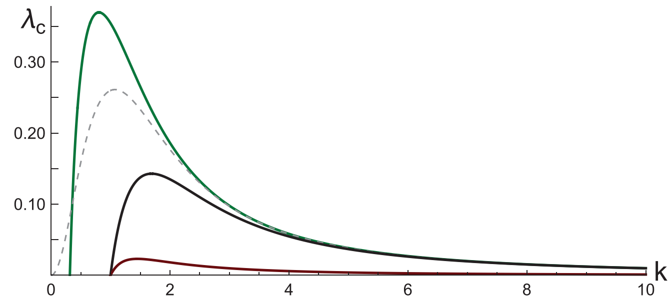

FIG. 1. Dispersion curves for the critical eigenvalue of the matrix $((-1 - k^2D_1, 2, 1), (-1, -k^2D_2, 0), (1, a_{32}, 0))^T$ under $a_{32} = 1$, $D_1 = D_2 = 1$ (black line); $a_{32} = 1$, $D_1 = 1$, $D_2 = 10$ (green line); $a_{32} = 1$, $D_1 = 10$, $D_2 = 1$ (red line); and $a_{32} = 0$, $D_1 = D_2 = 1$ (gray dashed line).

formation before a pattern is already close enough to its stable state. And when it is close to it, the small perturbations of the pattern, corresponding to great wave numbers, will die out instead of growing. Though being hard to prove analytically, such a concept can be illustrated via numerical simulations, which will be done in Sec. III.

Therefore, three-component network structures, in which the third element is immobile ($D_3 = 0$) and the following conditions for the types of interactions of the immobile element with itself and the mobile ones are met,

$$\begin{aligned}&a_{33} = 0,\\ &a_{13}a_{31} \geqslant 0, \quad a_{23}a_{32} \geqslant 0, \quad a_{13}a_{31} + a_{23}a_{32} > 0,\end{aligned} \tag{5}$$

are capable of producing classical Turing patterns if, as it was assumed, the homogeneous stationary state is stable in absence of diffusion and wave instability is not manifested simultaneously. Compliance with these requirements, however, in general still requires fine-tuning of the values of elements of matrix A. The following section is aimed at searching specific network structures for which these requirements can be met without fine-tuning.

B. Selecting network structures

1. Explanation of the concept

The main step toward solving the formulated problem is investigating the possibility that some three-component network structures that meet the conditions expressed in Eqs. (5) possess a certain interaction whose strength can be selected as a *control parameter* so that its increase over a certain threshold (by any amount, thus not requiring fine-tuning) will guarantee the stability of the matrix A and therefore the stability of the homogeneous stationary state of the corresponding system in absence of diffusion.

Due to the symmetries, implied by Eqs. (5), it is sufficient to consider $|a_{11}|$, $|a_{12}|$, and $|a_{13}|$ as candidates for control parameters. The cases of other parameters come down to one of these via relabeling variables u_1 and u_2 or/and applying mirror reflection of A with respect to its main diagonal or, in other words, changing the directions of all the mutual interactions within a network.

It is convenient to rewrite the conditions for stability of A, implied by Eq. (4), the following way:

$$-\sigma_0 = -a_{11} - a_{22} > 0, \tag{6a}$$

$$\Sigma_0 = a_{11}a_{22} - a_{12}a_{21} \overbrace{-a_{13}a_{31} - a_{23}a_{32}}^{<0} > 0, \tag{6b}$$

$$-\Delta_0 = a_{11}a_{23}a_{32} + a_{22}a_{13}a_{31}$$

$$- a_{12}a_{23}a_{31} - a_{13}a_{32}a_{21} > 0, \tag{6c}$$

$$- \sigma_0 \Sigma_0 + \Delta_0 > 0, \tag{6d}$$

where the second condition is excessive but convenient to be considered separately, since it is necessary for the fulfillment of the fourth condition. Each condition should be met either under any absolute values of all parameters or under any absolute values of noncontrol parameters and sufficiently high values of the control parameter. For brevity, theses cases will be referred to as situations, in which a condition *is met by itself* or *can be controlled*. It is easy to notice that for a condition to be met by itself each of its terms has to be positive, while for it to be able to be controlled, each of its terms that involves the highest power of the control parameter has to be positive. That means, in particular, that in any case all the terms that involve the highest power of the control parameter have to be positive and otherwise need to be nullified.

2. Rejecting parameters, unsuitable for control

It can be immediately seen that condition (6b) cannot be met by itself since, according to Eqs. (5), $-(a_{13}a_{31} + a_{23}a_{32})$ is always strictly negative. Moreover, $|a_{13}|$ therefore cannot act as the control parameter.

If $|a_{11}|$ is considered as the control parameter, then from condition (6a) it follows that a_{11} has to be negative. Condition (6b) has to be controlled, and therefore $a_{22} < 0$. According to Eqs. (5), $a_{23}a_{32} \geqslant 0$, hence the condition (6c) cannot be controlled and has to be met by itself. Its first term has to be nullified, at least one of a_{23} and a_{32} being set equal to zero. According to the current conditions, $a_{22}a_{13}a_{31} \leqslant 0$, therefore, this term as well has to be nullified. But a_{22} is already strictly negative, thus at least one of a_{13} and a_{31} have to be set to zero. This reasoning leads to contradiction will the last condition in Eqs. (5). Therefore, $|a_{11}|$ cannot act as a control parameter. The only candidate left for this role is $|a_{12}|$, which can fit it under suitable network structures.

3. Search for suitable network structures

When $|a_{12}|$ is considered as the control parameter, the condition (6a) should be met by itself and thus $a_{11} \leqslant 0$, $a_{22} \leqslant 0$. For the condition (6b) to be controlled, $a_{12}a_{21}$ should be negative. The term $a_{12}a_{23}a_{31}$ is included with different signs in (6c) and (6d) as a part of Δ_0 with no higher powers of a_{12} being present. Therefore, this term has to be nullified. Without loss of generality, let us set $a_{23} = 0$; it comes down to the case of $a_{31} = 0$ by application of both mirror and relabeling symmetries, which eventually preserve the control parameter [both parameters cannot be set to zero simultaneously due to Eqs. (5)]. As a_{12} is now not included in the condition (6c), it has to be met by itself. It now contains two terms, that are yet nonzero: $a_{22}a_{13}a_{31}$ and $-a_{13}a_{21}a_{32}$. The first term is lower or

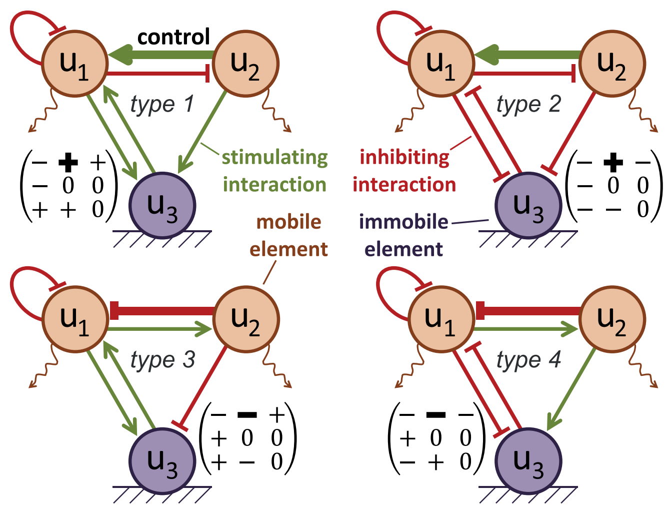

FIG. 2. Network structures that produce Turing instability under any values of kinetic parameters and diffusion coefficients of mobile elements under the increase of strength of the control interaction over a certain threshold, given by Eq. (7). Four more relevant structures can be obtained by mirror reflections of matrices with respect to main diagonals.

equal to zero and therefore has to be nullified. The only option to comply with Eqs. (5) is to set $a_{22} = 0$, due to which a_{11} has to be strictly negative. The remaining term in the condition (6c) now has to be positive. The only condition that now has be controlled is (6d), which can be done if

$$|a_{12}| > a_{\text{tr}} \equiv \left| \left[\frac{a_{31}}{a_{21}} + \frac{a_{32}}{a_{11}} \right] a_{13} \right|. \tag{7}$$

The validity of the condition (6b) follows from this inequality, as it infers $|a_{12}a_{21}| > |a_{13}a_{31}|$.

Overall, all the required conditions for the sought network structures are

$$a_{33} = 0, \;\; a_{23} = 0, \;\; a_{22} = 0, \;\; a_{11} < 0,$$

$$a_{12}a_{21} < 0, \;\; a_{13}a_{31} > 0, \;\; a_{13}a_{21}a_{32} < 0. \tag{8}$$

That results in four possible network structures, depicted in Fig. 2. Four more structures can be obtained by applying the mirror symmetry, discussed above (while relabeling symmetry merely leads to an identical structure). If the control parameter exceeds the threshold a_{tr}, given by Eq. (7), then the spatially homogeneous state becomes stable through a reverse Hopf bifurcation [since the condition (6c) is met by itself, while (6d) is controlled]. As it will be shown in the next section, wave instability cannot be manifested at least when (7) is met. Therefore, Turing instability destabilizes the waves with wave numbers

$$k > k_T \equiv \sqrt{\left| \frac{a_{21}a_{32}}{D_2 a_{31}} \right|}, \tag{9}$$

which follows from Eq. (3), this range being independent of the control parameter. Note that the decrease of $|a_{13}|$ under fixed values of other parameters should lead to the same result. However, from a practical point of view, such an option seems to be less attractive at least in noisy conditions and therefore is not considered.

4. Impossibility of simultaneous wave instability

As it follows from Eqs. (4) with account of Eqs. (8), the function that indicates the onset of wave instability under its nullification can be presented as a function, bicubic with respect to k^2: $\alpha k^6 + \beta k^4 + \gamma k^2 + \delta$, where

$$\alpha = -[D_1 + D_2]D_1 D_2,\ \beta = [2D_1 + D_2]D_2 a_{11},$$
$$\gamma = -D_2 a_{11}^2 + D_1[a_{12}a_{21} + a_{13}a_{31}] + D_2 a_{12}a_{21},$$
$$\delta = \sigma_0 \Sigma_0 - \Delta_0.$$

If $|a_{12}| > a_{\mathrm{tr}}$, then all its coefficients are strictly negative. Therefore, for $k^2 > 0$ it is a decreasing function with a negative value at $k^2 = 0$. Hence, it cannot be nullified and wave instability is thus impossible.

III. INVESTIGATION OF CONTROLLED TURING PATTERNS FORMATION

A. Random sampling of parameter sets

The first step of investigation of controlled Turing patterns formation under suggested network structures was the random sampling of relevant matrices $A = a_{ij}$ $(i, j = 1, 2, 3)$ and diffusion coefficients D_1, D_2 that would correspond to linearized dynamics of a yet unspecified system near its homogeneous stationary state. A thousand parameter sets were generated, 250 sets per every network structure, depicted in Fig. 2. The absolute values of parameters were represented as 10^n, where the exponents were independently and uniformly selected from the range $[-2, 1]$ for the kinetic parameters and $[-2, 2]$ for the diffusion coefficients. All parameter sets are listed in the Supplemental Material [34] along with the corresponding values of a_{tr}, k_T as well as the values of maximum linear growth rates $\lambda_M = \max \lambda_c(k)$ and corresponding wave numbers $k_M = \arg\max \lambda_c(k)$ at $|a_{12}| = a_{\mathrm{tr}}$, along with their statistics. The latter allows indicating the following deficiencies.

First, the range of λ_M occupies more than 10 orders of magnitude. This is important since sufficiently small linear growth rates are generally associated with slow formation of low-amplitude Turing patterns. Further, the values of k_M vary by almost five orders of magnitude, implying a great scatter in the characteristic lengths of corresponding patterns. The values of a_{tr} are also subject to significant variation, exceeding 100 in 8.5% of cases. More generally, it can be noticed that a universal approach toward guaranteed formation of Turing patterns under the considered restrictions on the parameter set should involve the increase of the control parameter up to the largest of its possible values, which, as it follows from Eq. (7), is 2×10^4. Notably, it can be shown that at $|a_{12}| > a_{\mathrm{tr}}$ $\forall k > k_T$ $\lambda_c(k)$ will monotonically decrease with the increase of the control parameter, and therefore λ_M will monotonically decrease as well. Furthermore, $k_M \to \infty$ as $|a_{12}| \to \infty$ (see Appendix A for the proofs). Hence, using the fixed value of $|a_{12}| = 2\times10^4$ should lead to even slower rates of pattern formation than estimated at $|a_{12}| = a_{\mathrm{tr}}$ and smaller characteristic lengths, increasing the chance that such patterns may not be discernible under realistic noisy conditions. It is possible to change the control parameter dynamically, with the final structure depending on the way of its change. However, a universal approach toward Turing patterns formation should still involve the increase of the control parameter up to 2×10^4, which may correspond to a quite unrealistic scale separation in a real system. The following section indicates a way to alleviate these problems.

B. Setting $a_{32} = 0$

From the statistical processing it follows that both k_M and λ_M show a strong correlation with k_T, thus implying that its decrease should be beneficial. It can be achieved by proper variation of four parameters in its formula [see Eq. (9)]. However, since the parameter values cannot be specified within a network structure, the only way to vary a parameter is to nullify it or to change its sign, the latter being of no use in this situation. Setting a_{21} to zero is useless, since it will at least require infinite threshold value for the control parameter, as follows from Eq. (7). Setting a_{32} to zero is therefore the only beneficial action that leads to nullification of k_T and transforms qualitatively the dispersion curve as shown in Fig. 1 via dashed line. Notably, it renders the uniform stationary state only marginally stable, formally leading to violation of one of the conditions for the network structures, listed in Eqs. (8). However, as it will be shown in the next section, at least in some systems this does not affect their ability to generate Turing patterns.

Furthermore, setting $a_{32} = 0$ simplifies the condition on the threshold value for the control parameter:

$$|a_{12}a_{21}| > |a_{13}a_{31}|,$$

and allows us to use both $|a_{12}|$ and $|a_{21}|$ as control parameters, *independent* in the general case. Given the above-mentioned restrictions on the parameter set, the spatially homogeneous state is marginally stable for any values of noncontrol parameters when both control parameters are greater than 10, which is the upper boundary of the range of kinetic parameters.

Setting $a_{32} = 0$ in the generated parameter sets significantly reduces the ranges of λ_M and k_M, estimated under $|a_{12}| = |a_{21}| = a_{Tr} \equiv \sqrt{a_{13}a_{31}}$, to slightly more than five orders of magnitude and less than three orders of magnitude correspondingly (see Supplemental Material [34]). Notably, under $a_{32} = 0$ mirror reflections do not lead to new network structures, thus resulting in overall four suitable types of them.

C. Selection of a specific system

All the reasoning provided above concerns linearized dynamics, while consideration of a specific system may significantly complicate the task of robust controlled formation of Turing patterns. First, the system may have another uniform stationary states, which may attract its dynamics, overriding Turing patterns formation. Moreover, even in the case of a single uniform stationary state its corresponding network structure can change depending on the parameter values—e.g., prevalence of self-activation over degradation and vice versa would result in different signs of a self-interaction. In this section it is shown that these difficulties can be overcome at least theoretically.

The considered system has the general form

$$\begin{aligned}\dot{u}_1 &= a_{11}u_1 + \eta_s a_c u_2 + a_{13}u_3 - u_1^3 + D_1 u_1'',\\ \dot{u}_2 &= -\eta_s a_c u_1 - u_2^3 + D_2 u_2'',\\ \dot{u}_3 &= a_{31}u_1 + a_{32}u_2 - u_3^3,\end{aligned} \quad (10)$$

where primes denote differentiation with respect to the sole space coordinate x, a_c is always positive for convenience, and the value of η_s depends on the network structure type s: $\eta_1 = \eta_2 = 1$, $\eta_3 = \eta_4 = -1$ (see Fig. 2). Note that (0,0,0) is the uniform stationary state under any parameter values. In the simulations only the cases with $a_{32} = 0$ will be considered; however, using this parameter explicitly in the general form is useful for the analysis.

Straightforward transformation of the equations allows us to obtain the expression for the coordinates u_2 of the uniform stationary states, which can be presented as

$$a_{32}u_2 + \eta_s\left\{-\frac{a_{31}}{a_c} + \left[\frac{a_c}{a_{13}}\right]^3\right\}u_2^3 + \sum_{j=2}^{13} K_j u_2^{2j+1} = 0, \quad (11)$$

where the signs of all the coefficients K_j coincide with the sign of $\eta_s[-1]^{s-1}$, i.e., they are all positive for $s = 1, 4$ and negative for $s = 2, 3$. When $a_c > a_{pf} \equiv \sqrt[4]{a_{13}^3 a_{31}}$, the cubic term with respect to u_2 has the same sign. As it may follow, e.g., from simple geometric reasoning, in this case Eq. (11) has one (zero) real root if the sign of a_{32} coincides with that indicated in Fig. 2 (which is also the sign of $\eta_s[-1]^{s-1}$) and three real roots otherwise. If $a_c < a_{pf}$, then there are still three real roots if $\mathrm{sgn} a_{32} \neq \mathrm{sgn}(\eta_s[-1]^{s-1})$; otherwise, there are five real roots under sufficiently small $|a_{32}|$ and one (zero) real root otherwise. It is easy to see that each of these roots can correspond to only one stationary state of the nondistributed system, corresponding to Eqs. (10). This suggests that it undergoes a pitchfork bifurcation when a_{32} changes its sign. It is subcritical if $a_c < a_{pf}$ and supercritical otherwise. If a_{32} is fixed to zero, then in the absence of diffusion the stationary state (0,0,0) is marginally stable under any value of a_c. Under $a_c > a_{pf}$ it is the only stationary state, while under $a_c < a_{pf}$ two more stable states exist.

As it follows from Eq. (7) and the reasoning provided in Sec. II B 3, in the absence of diffusion the uniform stationary state (0,0,0) of the system of Eqs. (10) undergoes Hopf bifurcation if $\mathrm{sgn} a_{32} = \mathrm{sgn}(\eta_s[-1]^{s-1})$ at

$$a_c = a_H \equiv -\frac{\eta_s a_{13}a_{32} + \sqrt{4a_{11}^2 a_{13}a_{31} + a_{13}^2 a_{32}^2}}{2a_{11}}. \quad (12)$$

Therefore, when $a_c < a_H$, state (0,0,0) is unstable. When $a_c > a_H$, it is stable, and depending on the type of Hopf bifurcation, either it is the only attractor $\forall a_c > a_H$ (supercritical case) or a stable periodic attractor as well persists under sufficiently low values of a_c (subcritical case). Numerical simulations suggest that such behavior maintains under $a_{32} = 0$ (when $a_H = a_{Tr} = \sqrt{a_{13}a_{31}}$). The type of Hopf bifurcation can be determined by weakly nonlinear analysis, which is performed in Appendix B.

All these features of the system of Eqs. (10) suggest that at $a_{32} = 0$ under sufficiently large values of a_c it will always have only one uniform stationary state, which is marginally stable in absence of diffusion, with no other attractors. Under the presence of diffusion the system will undergo Turing instability and only that, since wave instability is impossible (see Sec. II B 4). This makes this system a good candidate for numerical investigation, which is performed in the next section.

D. Numerical simulations

Numerical simulations were performed for all 1000 generated parameter sets in a one-dimensional domain of the length $L = 25$ with no-flux boundary conditions. Initial conditions corresponded to trivial uniform stationary state. The system was subjected to random low-amplitude noise. Splitting with respect to physical processes was used. During it, kinetic equations were solved by a Runge-Kutta fourth-order method and diffusion equations were solved by an implicit Crank-Nicholson method. Time and space steps were selected so that their decrease yielded no visible qualitative difference for the solutions. The simulations were run until $t = T = 3\times10^5$. For four parameter sets two-dimensional simulations were performed analogically, diffusion equations being solved using the alternating direction implicit method. The computational codes were implemented in C++ and can be found in the Supplemental Material along with the visualizations of all 1D simulations and their statistics [34].

At first a trivial control was implemented, i.e., using constant $a_c = 10$. In this case in 1D simulations at $t = T$ clearly visible Turing patterns were formed in 95.2% of cases. The use of a dynamic control $a_c(t) = \min(0.01\times10^{4t/T}, 10)$ increased the rate of pattern formation before $t = T$ to 99.7%, while it was checked that in the three remaining cases the patterns did form before $t = 2T$. In accordance with the theoretical reasoning, provided in Sec. III A, dynamic control on average yielded greater characteristic length of patterns, some of which were noticeably more regular. The number of individual structures N (determined roughly as half of the number of intersections of u_3 distribution with x axis) on average was ≈1.5 times less in the case of dynamic control. At that, the amplitude of patterns P (determined as half of the difference between maximum and minimum values of u_3) on average was less by ≈4%.

Figure 3 illustrates the process of Turing patterns formation under dynamic control in 1D in cases corresponding to four different network structures as well as the resulting patterns in 1D and the patterns obtained in 2D for the same parameter sets. For each of the network structures, depending on the parameter values, the process of patterns formation in 1D could be qualitatively different. For some of the parameter sets the patterns appeared before the passages of both Hopf bifurcation point (denoted via orange line) and the point where additional uniform stationary states disappeared (denoted via green line), like in Fig. 3(a). In other cases, like in Fig. 3(b), the system was at first attracted to one of these stable states. For some parameter sets uniform oscillations appeared transiently, and in some cases with subcritical Hopf bifurcation they affected pattern formation even after the

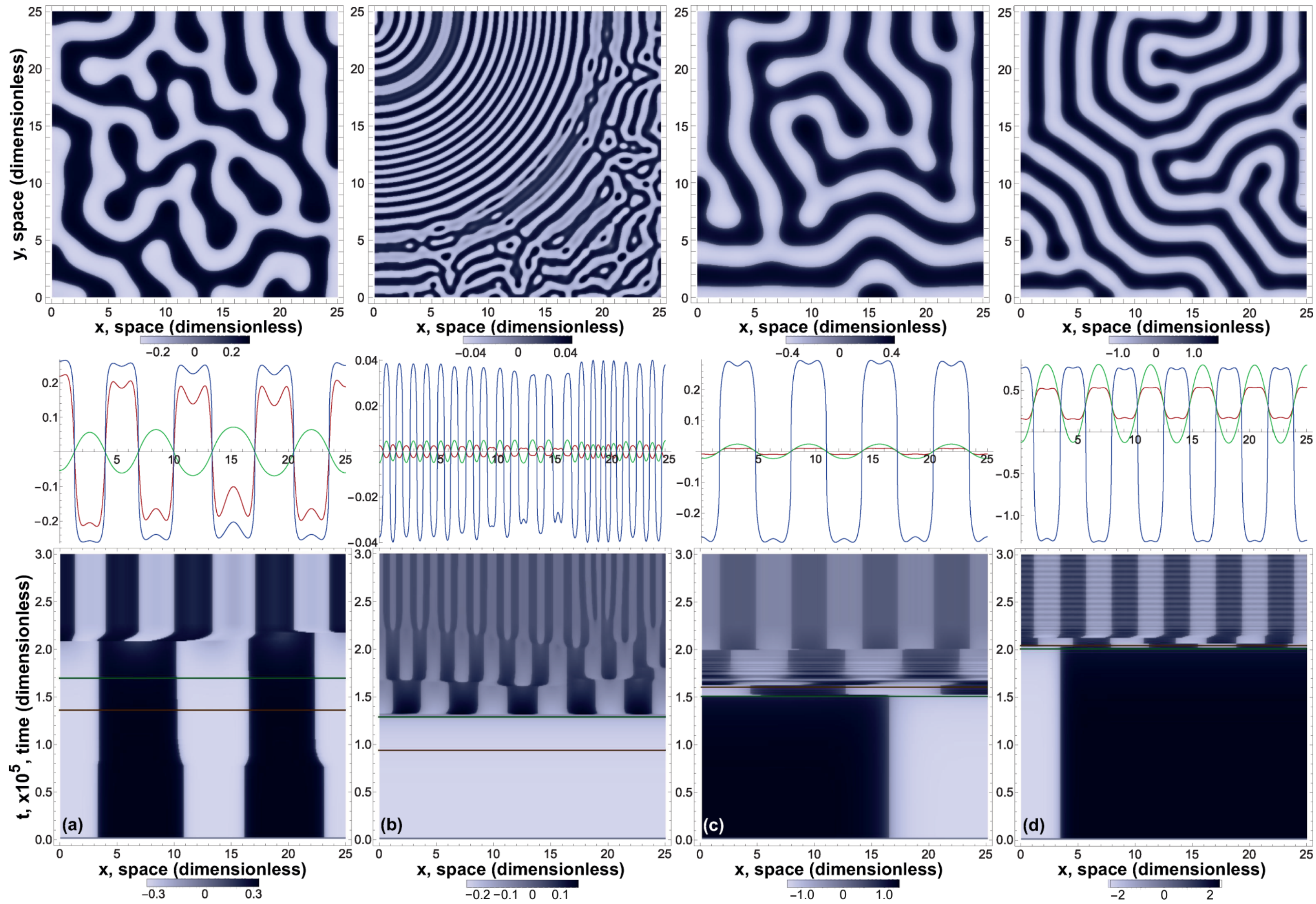

FIG. 3. Formation of Turing patterns in the systems: (a) $\dot u_1 = -3.657u_1 + a_c(t)u_2 + 5.133u_3 - u_1^3 + 0.294u_1''$, $\dot u_2 = -a_c(t)u_1 - u_2^3 + 32.661u_2''$, $\dot u_3 = 0.083u_1 - u_3^3$; (b) $\dot u_1 = -0.069u_1 + a_c(t)u_2 - 1.532u_3 - u_1^3 + 0.29u_1''$, $\dot u_2 = -a_c(t)u_1 - u_2^3 + 0.228u_2''$, $\dot u_3 = -0.021u_1 - u_3^3$; (c) $\dot u_1 = -0.075u_1 - a_c(t)u_2 + 0.759u_3 - u_1^3 + 2.588u_1''$, $\dot u_2 = a_c(t)u_1 - u_2^3 + 4.815u_2''$, $\dot u_3 = 2.492u_1 - u_3^3$; and (d) $\dot u_1 = -0.018u_1 - a_c(t)u_2 - 4.306u_3 - u_1^3 + 1.636u_1''$, $\dot u_2 = a_c(t)u_1 - u_2^3 + 2.252u_2''$, $\dot u_3 = -6.55u_1 - u_3^3$ under dynamic control parameter $a_c(t) = \min(0.01\times10^{4t/T}, 10)$, $T = 3\times10^5$. Lower pictures show evolutions of distribution of u_3, the green line denotes the moment at which pitchfork bifurcation changes its type from subcritical to supercritical, the orange line denotes the moment at which reverse Hopf bifurcation takes place, which is supercritical for (a) and (b) and subcritical for (c) and (d). Middle pictures demonstrate distributions of u_1 (red), u_2 (green), and u_3 (blue) at the moment T. Upper pictures show distributions of u_3 in the two-dimensional case at the moment T.

passage of its point, like in Fig. 3(c). Moderate oscillations of well-discernible nonhomogeneous patterns persisted until the end of some simulations, like in Fig. 3(d), thus yielding a mixed Turing-Hopf regime. Notably, all four variants of the phase relations between the variables were produced in the simulations, each one inherent to a certain network structure in accordance with the rules, deduced in Ref. [28].

Although Turing patterns eventually formed under all the parameter sets, their amplitudes varied by about three orders of magnitude and the numbers of their structures also differed substantially. Under dynamic control in five cases more than 100 structures fit into the computational region, while in seven cases only half of a structure emerged, which effectively divided the region into two parts of notably different levels of u_3. The following combinations of parameters, suggested by analytical results, showed a good correlation with the logarithms of amplitudes and number of structures correspondingly:

$$\alpha = \lg\left(\frac{D_2}{D_1}a_{13}a_{31}\right), \quad \nu = \lg\left(\frac{a_{13}a_{31}}{D_1 D_2}\right),$$

which is demonstrated in Fig. 4. This in particular suggests that despite formally overcoming the need for differential diffusivity, the increase of the ratio of diffusion coefficients D_2/D_1 should nevertheless be beneficial for the manifestation of patterns, which may be crucial under realistic noisy conditions.

IV. DISCUSSION

In physics and chemistry, experimental control of various spatiotemporal structures, including Turing patterns, is a popular area of research [35,36]. Generally, a control requires knowledge of the parameter values [37] or/and implementation of complex feedback schemes relying on ongoing system dynamics [38]. In this work, it was shown that in some systems with suitable sets of interactions between their elements Turing patterns formation can be guaranteed by a simple universal control under any values of parameters and in the absence of feedback loops that would rely on a system state.

This concept was illustrated by analysis and simulations of a simple three-component system. It was demonstrated that

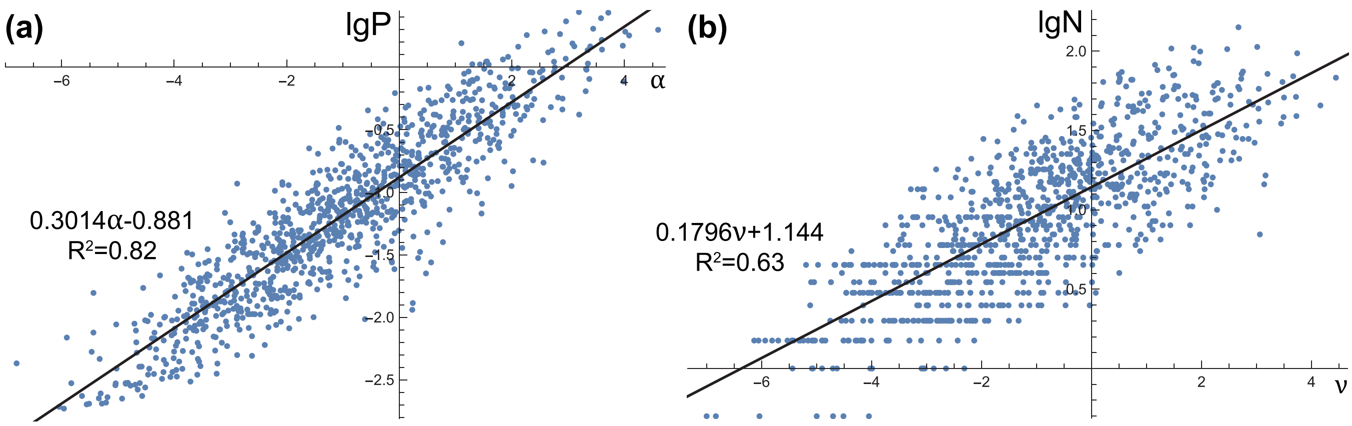

FIG. 4. Logarithm of (a) amplitudes P and (b) numbers N of Turing structures at the end of simulations of Eqs. (10) under control $a_c(t) = \min(0.01 \times 10^{4t/T}, 10)$ as functions of $\alpha = \lg(D_2 a_{13} a_{31}/D_1)$ and $\nu = \lg(a_{13} a_{31}/[D_1 D_2])$ correspondingly.

a smooth monotonic increase of the control parameter for the considered system should be more profitable in terms of probability of Turing patterns formation in finite time in the presence of external noise than just setting initially a sufficiently large value of the control parameter. This is due to the behavior of the dispersion curve with increase of the control parameter, discussed in Sec. III A, i.e., the decrease of maximum linear growth rate of spatially inhomogeneous patterns. From a biological point of view, such control may roughly correspond, e.g., to the inflow of an externally produced enzyme, or its production due to some epigenetic switch, in the area where Turing pattern formation is to take place, this enzyme influencing the strength of the control interaction in a corresponding network under the gradual increase of its concentration and thus overall acting as a trigger of the pattern formation.

Such a mechanism can be important for synthetic engineering, as it allows generating Turing patterns in certain networks by a simple universal control under any values of system parameters, which in relevant biological systems are often difficult to measure with desirable accuracy. Future work will focus on identification of analogical mechanisms in more complex and more realistic systems.

ACKNOWLEDGMENT

This paper has been supported by the RUDN University Strategic Academic Leadership Program.

APPENDIX A: BEHAVIOR OF $\lambda(k)$ ON INCREASE OF $|a_{12}|$

Let us recall the dispersion relation in the form

$$\lambda(k)^3 - \sigma(k)\lambda(k)^2 + \Sigma(k)\lambda(k) - \Delta(k) = 0,$$

its coefficients being defined by Eqs. (3). We consider a linearized system, corresponding to one of the network structures, depicted in Fig. 2, in a Turing regime, i.e., at $|a_{12}| > a_{\rm tr}$ [see Eq. (7)]. Therefore, $\forall k$ $\sigma(k) < 0$, $\Sigma(k) < 0$, while $\Delta(k) < 0$ for $k < k_T$ [see Eq. (9)] and $\Delta(k) > 0$ for $k > k_T$. Since $\Delta(k)$ changes its sign only once and no wave instability is possible (see Sec. II B 4), two noncritical eigenvalues have negative real parts for each k.

First, it can be seen from Eqs. (3) that $\Sigma(k)$ is the only coefficient that depends on $|a_{12}|$ and $\lim_{|a_{12}| \to +\infty} \Sigma(k) = +\infty$; moreover, $\Sigma(k)$ increases monotonically with increase of $|a_{12}|$. This infers that one of the eigenvalues, which can only be the critical eigenvalue, tends to zero $\forall k$ as $|a_{12}| \to +\infty$.

Now let us prove that at least when $k > k_T$ $\lambda_c(k)$ tends to zero monotonically. Let us increase $|a_{12}|$ by an arbitrarily value, denoting the corresponding increase of $\Sigma(k)$ as $d\Sigma(k)$ and new critical eigenvalue as $\mu_c(k)$. Since k_T does not depend on $|a_{12}|$, we can infer that $\mu_c(k) > 0$. We obtain:

$$\lambda_c(k)^3 - \sigma(k)\lambda_c(k)^2 + \Sigma(k)\lambda_c(k) - \Delta(k) = 0,$$
$$\mu_c(k)^3 - \sigma(k)\mu_c(k)^2 + [\Sigma(k) + d\Sigma(k)]\mu_c(k) - \Delta(k) = 0.$$

Subtracting the second equation from the first leads to

$$\{\overbrace{\lambda_c(k)^2 + \lambda_c(k)\mu_c(k) + \mu_c(k)^2}^{>0} \overbrace{-\sigma(k)[\lambda_c(k) + \mu_c(k)]}^{>0} \overbrace{+\Sigma(k)}^{>0}\}[\lambda_c(k) - \mu_c(k)] = \overbrace{d\Sigma_k \mu_c(k)}^{>0},$$

and this inequality can be met only if $\mu_c(k) < \lambda_c(k)$, which infers the proof of the considered proposition.

Finally, let us show that $k_M = \arg\max \lambda_c(k) \to \infty$ as $|a_{12}| \to \infty$. It can be straightforwardly checked that for the eigenvalues the following relations hold:

$$\lambda_c(k) = \Delta(k)/[\lambda_2(k)\lambda_3(k)],$$
$$\lambda_2(k) + \lambda_3(k) = \sigma(k) - \lambda_c(k),$$
$$\lambda_2(k)\lambda_3(k) + \lambda_c(k)[\lambda_2(k) + \lambda_3(k)] = \Sigma(k).$$

It is known that $\forall |a_{12}|$ $\lambda_c(k) \to +0$ as $k \to \infty$, form which it follows that $\lambda_2(k) + \lambda_3(k) \to \sigma(k)$. Using this, it is easy to obtain a quadratic equation for the limit of the product of two noncritical eigenvalues, which leads to (accounting for the fact that it should be positive):

$$\lim_{k\to\infty} \lambda_2(k)\lambda_3(k) = \tfrac{1}{2}[\Sigma(k) + \sqrt{\Sigma(k)^2 - 4\Delta(k)\sigma(k)}].$$

Apparently, $\forall k$ as $|a_{12}| \to \infty$ this expression tends to $\Sigma(k)$, hence, $\lambda_c(k) \to \Delta(k)/\Sigma(k)$. Straightforward calculations indicate that the maximum of this function is achieved at $k = \sqrt[4]{-[a_{12}a_{21} + a_{13}a_{31}]/[D_1D_2]}$, which tends to infinity as $|a_{12}| \to \infty$, confirming the considered proposition.

APPENDIX B: DETERMINING HOPF BIFURCATION TYPE

The type of Hopf bifurcation of the stationary state (0,0,0) of the system of Eqs. (10) in absence of diffusion can be determined via a multiscale technique, which is described, e.g., in Ref. [39].

Let us represent the system in the following form:

$$\frac{d}{dt}\overbrace{\begin{pmatrix} u_1 \\ u_2 \\ u_3 \end{pmatrix}}^{\mathbf{u}} = \overbrace{\begin{pmatrix} a_{11} & \eta_s a_c & a_{13} \\ -\eta_s a_c & 0 & 0 \\ a_{31} & a_{32} & 0 \end{pmatrix}}^{\mathscr{L}(a_c)}\mathbf{u} - \overbrace{\begin{pmatrix} u_1^3 \\ u_2^3 \\ u_3^3 \end{pmatrix}}^{\mathbf{h}(\mathbf{u})}.$$

The critical value of the control parameter a_c for Hopf bifurcation, a_H, is given in Eq. (12). Note that Hopf bifurcation takes place as a_c is decreased. The decomposition of variables with respect to auxiliary smallness parameter ϵ has the following form:

$$\mathbf{u} = \epsilon\mathbf{u_I} + \epsilon^2\mathbf{u_2} + \epsilon^3\mathbf{u_3} + \cdots,$$
$$a_c - a_H = \epsilon^2\gamma_2 + \cdots,$$
$$\frac{d}{dt} = \Omega_H\frac{d}{dT} + \epsilon^2\frac{d}{d\tau} + \cdots$$

where Ω_H is the imaginary part of the critical eigenvalue of $\mathscr{L}(a_H)$:

$$\Omega_H = \sqrt{\frac{-\eta_s a_{13}a_{32}}{a_{11}}a_H}.$$

Note that the linear terms in the decompositions of $a_c - a_H$ and d/dt are known to be equal to zero for Hopf instability.

To the first order of ϵ we obtain the following equation:

$$\left[\mathscr{L}(a_H) - \Omega_H\frac{d}{dT}\right]\mathbf{u_I} = 0. \tag{B1}$$

We seek a solution in the form

$$\mathbf{u_I} = c(\tau)\mathbf{v}e^{iT} + cc,$$

where $c(\tau)$ is its amplitude. Up to a factor $\mathbf{v}$ is equal to

$$\mathbf{v} = \begin{pmatrix} \Omega_H^2/[\eta_s a_{32}a_H - ia_{31}\Omega_H] \\ -a_H\Omega_H/[\eta_s a_{31}\Omega_H + ia_{32}a_H] \\ 1 \end{pmatrix}.$$

Since $\mathbf{h_{uu}}(\mathbf{u})$ is a zero vector, the equation for the second order of ϵ coincides with Eq. (B1). Its solution nevertheless in not included in the equation for the third order of ϵ, which is

$$\left[\mathscr{L}(a_H) - \Omega_H\frac{d}{dT}\right]\mathbf{u_{III}} = -\gamma_2\mathscr{L}'_{a_c}\mathbf{u_I} + \mathbf{u_I}^3 + \frac{d\mathbf{u_I}}{d\tau} = \mathbf{q_{III}}.$$

According to the theorem of the Fredholm alternative, the following condition should be met in order for the solution of this equation to exist:

$$\int_0^{2\pi}\mathbf{v}^+\cdot\mathbf{q_{III}}dT = 0, \tag{B2}$$

where $\mathbf{v}^+$ is the null eigenvector of

$$\mathscr{L}^+(a_H) = \begin{pmatrix} a_{11} + i\Omega_H & -\eta_s a_H & a_{31} \\ \eta_s a_H & i\Omega_H & a_{32} \\ a_{13} & 0 & i\Omega_H \end{pmatrix},$$

which is up to a factor

$$\mathbf{v}^+ = \begin{pmatrix} -i\Omega_H/a_{13} \\ \eta_s[\Omega_H^2 - ia_{11}\Omega_H + a_{13}a_{31}]/[a_{13}a_H] \\ 1 \end{pmatrix}.$$

In Eq. (B2) nonzero contributions on integration are given only by terms of $\mathbf{q_{III}}$ that contain the factor e^{iT}. With account of this, straightforward calculations lead to the equation of the following form, where $z = \epsilon c$:

$$\frac{\partial z}{\partial t} = (a_c - a_H)P_1 z + P_3|z|^2 z,$$

the general expressions for P_1 and P_3 being quite cumbersome. Our goal, however, is only to determine the type of bifurcation at $a_{32} = 0$, which follows from the sign of

$$\lim_{a_{32}\to 0}\frac{\mathrm{Re}(P_1)}{\mathrm{Re}(P_3)} = -\frac{2}{3}\frac{a_{11}a_{31}\sqrt{a_{13}a_{31}}}{a_{11}^2[3a_{13} + a_{31}] + a_{13}a_{31}[a_{13} - a_{31}]}.$$

When this expression is positive, the system undergoes subcritical bifurcation and otherwise a supercritical one.

[1] A. M. Turing, The chemical basis of morphogenesis, Philos. Trans. R. Soc. Lond. B **237**, 37 (1952).

[2] A. Nakamasu, G. Takahashi, A. Kanbe, and S. Kondo, Interactions between zebrafish pigment cells responsible for the generation of Turing patterns, Proc. Natl. Acad. Sci. USA **106**, 8429 (2009).

[3] J. Raspopovic, L. Marcon, L. Russo, and J. Sharpe, Digit patterning is controlled by a Bmp-Sox9-Wnt Turing network modulated by morphogen gradients, Science **345**, 566 (2014).

[4] J. C. Scoones and T. W. Hiscock, A dot-stripe Turing model of joint patterning in the tetrapod limb, Development **147**, dev183699 (2020).

[5] V. K. Vanag and I. R. Epstein, Resonance-induced oscillons in a reaction-diffusion system, Phys. Rev. E **73**, 016201 (2006).

[6] M. Kuznetsov, A. Kolobov, and A. Polezhaev, Pattern formation in a reaction-diffusion system of Fitzhugh-Nagumo type before the onset of subcritical Turing bifurcation, Phys. Rev. E **95**, 052208 (2017).

[7] S. Mimar, M. M. Juane, J. Park, A. P. Munuzuri, and G. Ghoshal, Turing patterns mediated by network topology in homogeneous active systems, Phys. Rev. E **99**, 062303 (2019).

[8] V. Ardizzone, P. Lewandowski, M.-H. Luk, Y.-C. Tse, N.-H. Kwong, A. Lücke, M. Abbarchi, E. Baudin, E. Galopin, J. Bloch

et al., Formation and control of Turing patterns in a coherent quantum fluid, Sci. Rep. **3**, 3016 (2013).

[9] P. Rumbach, A. E. Lindsay, and D. B. Go, Turing patterns on a plasma-liquid interface, Plasma Sources Sci. Technol. **28**, 105014 (2019).

[10] H. Bao, L. Olivieri, M. Rowley, S. T. Chu, B. E. Little, R. Morandotti, D. J. Moss, J. S. Totero Gongora, M. Peccianti, and A. Pasquazi, Turing patterns in a fiber laser with a nested microresonator: Robust and controllable microcomb generation, Phys. Rev. Res. **2**, 023395 (2020).

[11] V. K. Vanag and I. R. Epstein, Diffusive instabilities in heterogeneous systems, J. Chem. Phys. **119**, 7297 (2003).

[12] M. Dolnik, T. Bánsági, S. Ansari, I. Valent, and I. R. Epstein, Locking of Turing patterns in the chlorine dioxide–iodine–malonic acid reaction with one-dimensional spatial periodic forcing, Phys. Chem. Chem. Phys. **13**, 12578 (2011).

[13] I. L. Mallphanov and V. K. Vanag, Distance dependent types of coupling of chemical micro-oscillators immersed in a water-in-oil microemulsion, Phys. Chem. Chem. Phys. **23**, 9130 (2021).

[14] M. B. Short, P. J. Brantingham, A. L. Bertozzi, and G. E. Tita, Dissipation and displacement of hotspots in reaction-diffusion models of crime, Proc. Natl. Acad. Sci. USA **107**, 3961 (2010).

[15] P. F. Pelz, J. Friesen, and J. Hartig, Similar size of slums caused by a Turing instability of migration behavior, Phys. Rev. E **99**, 022302 (2019).

[16] A. Zincenko, S. Petrovskii, V. Volpert, and M. Banerjee, Turing instability in an economic–demographic dynamical system may lead to pattern formation on a geographical scale, J. R. Soc. Interface. **18**, rsif.2021.0034 (2021).

[17] N. S. Scholes and M. Isalan, A three-step framework for programming pattern formation, Curr. Opin. Chem. Biol. **40**, 1 (2017).

[18] G. M. Kozubov and A. I. Taskaev, Characteristics of morphogenesis and growth processes of conifers in the Chernobyl nuclear accident zone, Radiatsion. Biol. Radioecolog. **47**, 204 (2007).

[19] A. M. Nesterenko, M. B. Kuznetsov, D. D. Korotkova, and A. G. Zaraisky, Morphogene adsorption as a Turing instability regulator: Theoretical analysis and possible applications in multicellular embryonic systems, PLoS ONE **12**, e0171212 (2017).

[20] V. Castets, E. Dulos, J. Boissonade, and P. De Kepper, Experimental Evidence of a Sustained Standing Turing-Type Nonequilibrium Chemical Pattern, Phys. Rev. Lett. **64**, 2953 (1990).

[21] R. Sekine, S. Tatsuo, and M. Ebisuya, Synthetic mammalian pattern formation driven by differential diffusivity of Nodal and Lefty, Nat. Commun. **9**, 5456 (2018).

[22] B. Borek, J. Hasty, and L. Tsimring, Turing patterning using gene circuits with gas-induced degradation of quorum sensing molecules, PLoS ONE **11**, e0153679 (2016).

[23] P. A. Haas and R. E. Goldstein, Turing's Diffusive Threshold in Random Reaction-Diffusion Systems, Phys. Rev. Lett. **126**, 238101 (2021).

[24] T. Biancalani, F. Jafarpour, and N. Goldenfeld, Giant Amplification of Noise in Fluctuation-Induced Pattern Formation, Phys. Rev. Lett. **118**, 018101 (2017).

[25] D. Karig, K. M. Martini, T. Lu, N. A. DeLateur, N. Goldenfeld, and R. Weiss, Stochastic Turing patterns in a synthetic bacterial population, Proc. Natl. Acad. Sci. USA **115**, 6572 (2018).

[26] L. Marcon, X. Diego, J. Sharpe, and P. Müller, High-throughput mathematical analysis identifies Turing networks for patterning with equally diffusing signals, Elife **5**, e14022 (2016).

[27] M. M. Zheng, B. Shao, and Q. Ouyang, Identifying network topologies that can generate Turing pattern, J. Theor. Biol. **408**, 88 (2016).

[28] X. Diego, L. Marcon, P. Müller, and J. Sharpe, Key features of Turing systems are determined purely by network topology, Phys. Rev. X **8**, 021071 (2018).

[29] N. S. Scholes, D. Schnoerr, M. Isalan, and M. P. Stumpf, A comprehensive network atlas reveals that Turing patterns are common but not robust, Cell Syst. **9**, 243 (2019).

[30] M. Kuznetsov and A. Polezhaev, Widening the criteria for emergence of Turing patterns, Chaos **30**, 033106 (2020).

[31] M. Dolnik, A. B. Rovinsky, A. M. Zhabotinsky, and I. R. Epstein, Standing waves in a two-dimensional reaction- diffusion model with the short-wave instability, J. Phys. Chem. A **103**, 38 (1999).

[32] A. Marciniak-Czochra, G. Karch, and K. Suzuki, Instability of Turing patterns in reaction-diffusion-ODE systems, J. Math. Biol. **74**, 583 (2017).

[33] F. R. Gantmacher and J. L. Brenner, *Applications of the Theory of Matrices* (Courier Corporation, New York, 2005).

[34] See Supplemental Material at http://link.aps.org/supplemental/10.1103/PhysRevE.105.014209 for the list of parameter sets, their statistics, the code for numerical simulations and their visualizations and statistics.

[35] A. S. Mikhailov and K. Showalter, Control of waves, patterns and turbulence in chemical systems, Phys. Rep. **425**, 79 (2006).

[36] G.-L. Oppo, Formation and control of Turing patterns and phase fronts in photonics and chemistry, J. Math. Chem. **45**, 95 (2009).

[37] R. McIlwaine, V. K. Vanag, and I. R. Epstein, Temperature control of pattern formation in the Ru(bpy)32+-catalyzed BZ-AOT system, Phys. Chem. Chem. Phys. **11**, 1581 (2009).

[38] R. Martin, A. J. Scroggie, G.-L. Oppo, and W. J. Firth, Stabilization, Selection, and Tracking of Unstable Patterns by Fourier Space Techniques, Phys. Rev. Lett. **77**, 4007 (1996).

[39] G. Nicolis, *Introduction to Nonlinear Science* (Cambridge University Press, Cambridge, UK, 1995).